

# The Adam Database and its Potential to Investigate High Temporal Sampling Acquisition at High Spatial Resolution for the Monitoring of Agricultural Crops

Frédéric Baret, R. Vintilă, C. Lazăr, N. Rochdi, L Prevot, Jean-Claude Favard, H. de Boissezon, Claire Lauvernet, E. Petcu, G Petcu, et al.

## ► To cite this version:

Frédéric Baret, R. Vintilă, C. Lazăr, N. Rochdi, L Prevot, et al.. The Adam Database and its Potential to Investigate High Temporal Sampling Acquisition at High Spatial Resolution for the Monitoring of Agricultural Crops. Romanian Agricultural Research, 2001, 16, pp.69-80. hal-03039097

**HAL Id: hal-03039097**

**<https://hal.inrae.fr/hal-03039097>**

Submitted on 3 Dec 2020

**HAL** is a multi-disciplinary open access archive for the deposit and dissemination of scientific research documents, whether they are published or not. The documents may come from teaching and research institutions in France or abroad, or from public or private research centers.

L'archive ouverte pluridisciplinaire **HAL**, est destinée au dépôt et à la diffusion de documents scientifiques de niveau recherche, publiés ou non, émanant des établissements d'enseignement et de recherche français ou étrangers, des laboratoires publics ou privés.

# THE ADAM DATABASE AND ITS POTENTIAL TO INVESTIGATE HIGH TEMPORAL SAMPLING ACQUISITION AT HIGH SPATIAL RESOLUTION FOR THE MONITORING OF AGRICULTURAL CROPS

F. Baret<sup>1</sup>, R. Vintilă<sup>2</sup>, C. Lazăr<sup>3</sup>, N. Rochdi<sup>1</sup>, L. Prévot<sup>1</sup>, J.C. Favard<sup>4</sup>, H. de Boissezon<sup>4</sup>,  
C. Lauvernet<sup>1</sup>, E. Petcu<sup>3</sup>, G. Petcu<sup>3</sup>, P. Voicu<sup>2</sup>, J. P. Denux<sup>6</sup>, V. Poenaru<sup>5</sup>, O. Marloie<sup>1</sup>,  
C. Simota<sup>2</sup>, C. Radnea<sup>2</sup>, D. Turnea<sup>2</sup>, F. Cabot<sup>4</sup>, P. Henry<sup>4</sup>

## ABSTRACT

The ADAM project (Assimilation of Spatial Data within Agriculture Models) was aiming at the development and evaluation of methods capable of exploiting high revisit frequency and high spatial satellite observations. The intensive experimental campaign conducted in 2000–2001 over wheat crops yielded a unique database where frequent satellite observations at high spatial resolution in the solar and microwave domains were made concurrently to ground characterization of the soil and the canopy and their functioning. This includes 39 SPOT images, 15 Radar (ERS and RadarSat) images, soil permanent characterization, frequent canopy leaf area index, biomass, soil water and nitrogen contents, as measured over 42 elementary sampling units (ESU). This intensive campaign will be followed in 2002 and 2003 by lighter campaigns where a reduced number of ESUs will be sampled, and a reduced number of SPOT scenes will be acquired. The objective of this paper is to present the ADAM experiment and the database generated, along with few examples illustrating its potentials. The ADAM database, freely accessible to the scientific community, is also described. Finally, conclusions are drawn on the problems associated to the exploitation of dense time series of images acquired by different sensors. A discussion is made on the potential exploitation of such a database.

**Key words:** biomass, LAI, radar, reflectance, remote sensing, revisit frequency, soil moisture, spatial resolution wheat, yield.

## INTRODUCTION

Remote sensing offers a potentially very appealing tool for the monitoring of vegetation over large areas that could benefit a wide range of applications. This is the case for agriculture, where increasing emphasis is put on the process of decision making that should incorporate as much information as available. This in-

cludes the several constraints the farmers are facing, either economical or logistical ones, but also environmental constraints that should be accounted for to reach sustainable agriculture systems. The information on the spatial variability observed within and between fields is critical. It encompasses the soil permanent characteristics such as soil texture and organic matter content, but also the state of the canopy that could be assessed from observations of few biophysical variables such as the leaf area index (LAI) and the chlorophyll content. Canopy state assessment should be made at regular intervals during the growth cycle depending on the cultural practices to be accommodated on the crops. In addition to this local scale application associated to a spatial resolution in between 5–20 m, other applications require the same type of satellite information. They correspond to the crop production estimation that is achieved at the level of a field, farms or a cluster of farms, sharing the same storage and trading facilities. It is also the case for governmental organizations that will soon be asked to report about the environmental status of a given region under the pressure of specific land use. In addition to these diagnostic reports, prognostic assessment under a range of land use scenarios has also to be completed. This could be only achievable by exploiting integrated process models describing the functioning of the landscape. Because of the complexity of such models, proper calibration and validation processes should be developed before being able to

<sup>1</sup> NRA-CSE, Avignon, France (baret@avignon.inra.fr)

<sup>2</sup> RISSA/ICPA, Bucharest, Romania (rvi@icpa.ro)

<sup>3</sup> RICIC, Fundulea, Romania (lazar@ricic.ro)

<sup>4</sup> CNES, Toulouse, France (Jean-Claude.Favard@cnes.fr)

<sup>6</sup> ROSA/ASR, Bucharest, Romania (violeta.poenaru@rosa.ro)

<sup>5</sup> ESAP, Toulouse, France (jpdenux@esa-purpan.fr)

use these models in a prognostic mode. Remote sensing observations could play here a key role by providing an elegant way of calibrating and validating such models through comparison of simulated and observed biophysical variables such as LAI.

However, one of the most stringent limitations of such approaches is the current lack of dedicated sensors that allow making frequent observations at a spatial resolution consistent with the size of heterogeneities within fields. Such space missions are being prepared, mostly focusing on the environmental applications and the related science questions, particularly regarding the carbon and water cycles (Dedieu et al., 1999; Rast et al., 2001).

In the framework of the preparation of such future missions, better knowledge has to be acquired on the way remote sensing observations could feed process models describing the functioning of the surface. For this reason, CNES (French Space Agency) decided to develop a specific project, ADAM: Assimilation of Spatial Data within Agriculture Models. This

project is based on a comprehensive experiment where high spatial and temporal resolution data acquired over an agriculture area during the whole crop growing season will complement ground characterization of the soil and the crop. This will ultimately allow evaluating remote sensing data assimilation techniques with emphasis on the temporal requirements and associated accuracy of outputs such as production estimation.

The objective of this paper is to present the experiment that took place in Romania from October 2000 to July 2001 over wheat crops.

## 2. The ADAM Experiment

### 2.1. Site description

The ADAM site ( $44^{\circ}27'38.43''\text{N}$ ;  $26^{\circ}37'14.34''\text{E}$ ) is a  $20 \times 20 \text{ km}^2$  area situated close to the Fundulea town in Romania, at about 30 km East from Bucharest (Figure 1). This particular location was selected because it corresponded to an area of intensive agriculture,

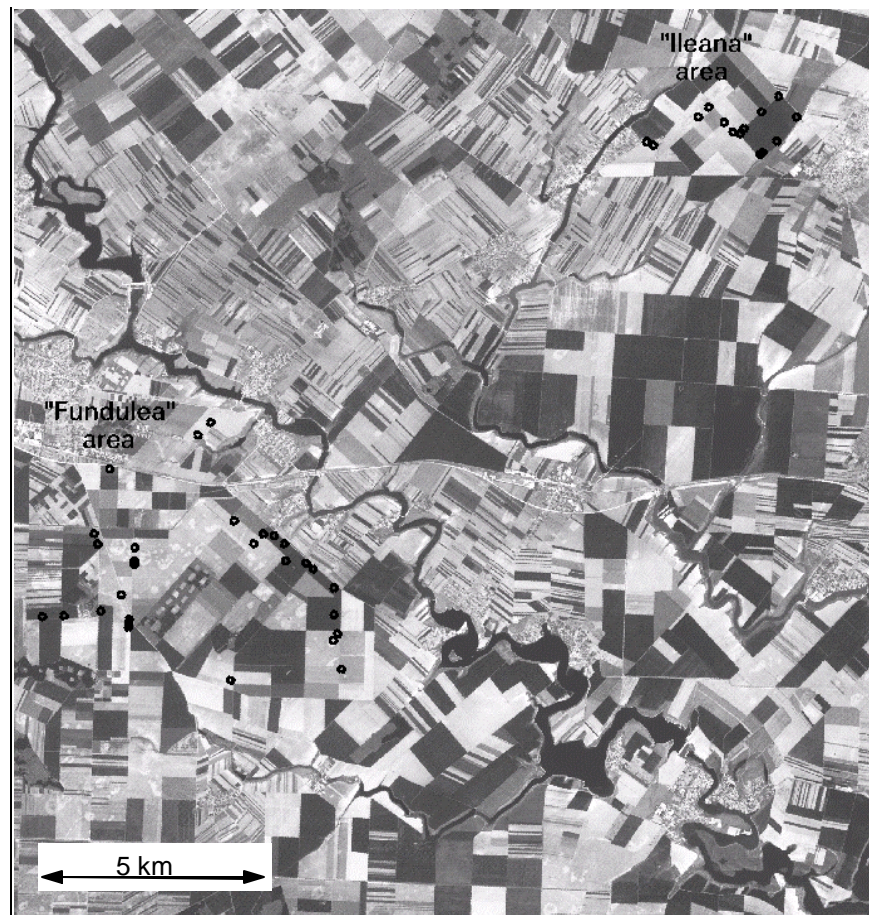


Figure 1. Panchromatic SPOT image of the ADAM site. The small circles represent the location of the elementary sampling units

where SPOT1, SPOT2 and SPOT4 satellites could complement each other to provide the required high temporal revisit frequency targeted.

Agriculture represents most of the land use, although few patches of broad leaved-forests remain in some places. The seed production farms of the R.I.C.I.C. Fundulea have large wheat fields with area between 15 ha and 40 ha on which the experiment took place. Apart from wheat, the main crops are maize, sunflower, barley, peas, soybeans, chickpeas, oats, sorghum, flax and alfalfa. The area sampled was concentrated in two zones: Fundulea, which was the main area investigated, and Ileana, at the Northern-East part of the site (Figure 1).

The topography is generally flat, with a mean elevation of about 55 m. Only a very limited fraction of the area corresponds to significant slopes bordering the small rivers. Several closed micro-depressions („crov”) are observed and may induce some local variation in soil properties and functioning. Cambic and Argiluvic Chernozem soils dominate, leading to quite uniform soil characteristics. However cropping techniques used during the last 50 years have significantly influenced its physical and chemi-

induce variation in the crop growth. The intensive experiment lasted from October 2000 to July 2001. Complementary campaigns will be conducted up to 2003.

## 2.2. Climatic and atmospheric conditions

### 2.2.1. Meteorological measurements

During the whole experiment, the meteorological data were measured with an automated station placed in the Fundulea area. The following variables were measured every 15 minutes: rainfall, air temperature at 2 m height, soil temperature profile (at 2, 5, 10, 25, 50 and 100 cm depth), relative air humidity, wind speed and direction at 2 m height, and global radiation. The 2000-2001 growing season was characterized by a very dry autumn and winter, with almost no snow cover and significantly higher temperatures than usual (Figure 2). The spring was relatively wet, with temperatures close to the usual values. These climatic conditions were generally favourable for the wheat growth. This explains why no irrigation was applied to the crops this year. Note that the climatic conditions were also very favourable for satellite acquisitions in the optical domain due to a lower number of cloudy days, particularly

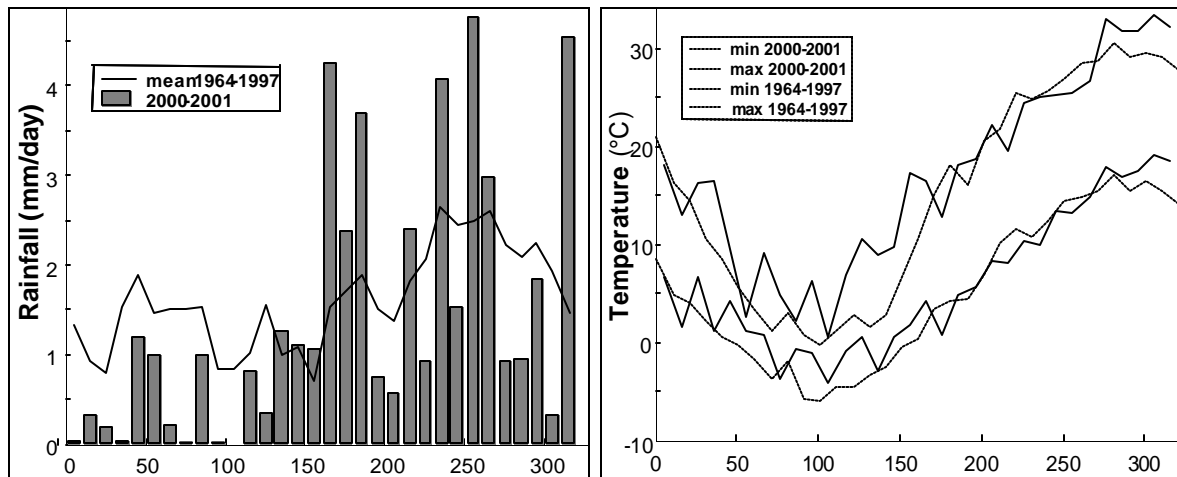


Figure 2. Decadal rainfall and temperature time course during the campaign year 2000–2001 as compared to the mean decadal values observed over the 1964–1997 period. The temporal scale is expressed in days since the first of October 2000

cal characteristics (Canarache, 2002) and may

in the winter season.

### 2.2.2. Atmosphere characterization

A CIMEL automatic sun-photometer connected to the AERONET network (Holben et al., 1998) was installed on the roof of the RICIC main building. It allowed characterizing the aerosol types and optical depth during the whole experiment. This was mandatory for the atmospheric corrections of the optical sensors. The data are available at:

<http://aeronet.gsfc.nasa.gov/>.

In addition, a direct and diffuse PAR device (BF2, delta-T device <http://www.delta-t.co.uk/frame/submenu/bf2ref.html>) was installed close to the meteorological station. This was used as a back up instrument for the estimation of the aerosol optical depth in case of failure of the sun-photometer.

### 2.3. Remotely sensed data

Both optical and microwave sensors were used to get the maximum information on the canopy and soil state variables. The satellite characteristics and temporal sampling scheme will first be presented. Then, the pre-processing applied to the data to get consistent top of canopy registered and calibrated reflectance and backscattering coefficients will be described.

#### 2.3.1. Satellite instruments and observation temporal sampling

Table 1 presents the main characteristics of the satellite instruments used during the intensive ADAM experiment. The high temporal sampling acquisition was routinely achieved by the concurrent use of three SPOT 1, 2 and 4 satellite sensors. A total of 39 almost cloud free SPOT XS images were acquired between October 2000 and July 2001. In addition, 5 SPOT XS images will be acquired in 2002 and other acquisitions are planned in 2003. In the micro-

wave domain, 14 radar (ERS and RadarSat) images have been acquired in 2000–2001. This corresponded to 8 ERS-2 SAR (C-band, 23°, VV) images with a gap between December 2000 and April 2001 because of technical problems aboard ERS 2 satellite. Then, 6 RadarSat SAR (C-band, HH) images were acquired in the „low incidence mode” (16° incidence angle) thanks to its multi-angular capability. This particular configuration was chosen to minimize the effect of the soil roughness, as well as the signal attenuation by the vegetation. Both SAR data were acquired in single look complex mode.

#### 2.3.2. Satellite image pre-processing

Because of remote sensing data temporal series will be integrated within process models, very accurate registration and calibration of the sensors should be performed. This was achieved according to:

**Registration of images.** The satellite images were projected over the Gauss-Krüger projection system for „zone 5” on the Krasovsky ellipsoid. To ensure a high level of consistency of the registration between the images, a SPOT XS image of 20 x 20 m<sup>2</sup> spatial resolution was used as a common reference. This reference image was itself registered to 20 well identified ground control points that were precisely located at the ground level using very accurate differential GPS (rms < 1 cm). The co-registration with other SPOT images was obtained by using spatio-triangulation techniques and a digital elevation model. Results show performances around rms ~ 0.5 pixel for the whole SPOT scene (60 x 60 km<sup>2</sup>). Radar images were geometrically corrected using the orbit descriptors and a digital elevation model, then re-sampled at 20 x 20 m<sup>2</sup> to be consistent with the

Table 1. Main characteristics of the satellite instruments used during the ADAM experiment

Sensor	Satellite	Number of bands & spectral domain	Spatial sampling	Revisit frequency	Swath width	View zenith angle	Polarization
HRV-XS	SPOT 1 SPOT 2	VNIR (3)	20 m	3 days	60 km	± 27° across-track	no
HRVIR	SPOT 4 SPOT 5	VNIR (3) SWIR (1)					
ERS 2		C-band	20 m	16 days	100 km	23°	VV
RadarSat		C-band	20 m	24 days	170 km	16°	HH

reference SPOT image (Figure 3).

## 2.4. Ground measurements

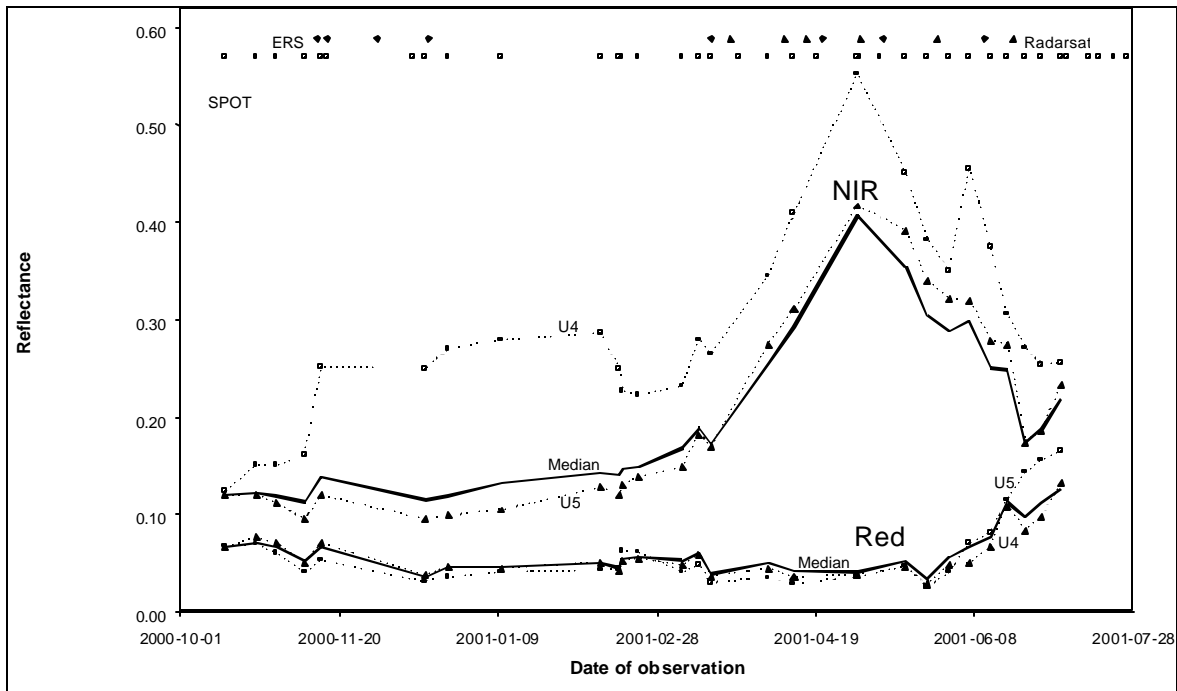


Figure 3. Temporal sampling of satellite observations over the ADAM site. The bottom graphs correspond to the red (Red) and near infrared (NIR) top of canopy reflectance as derived from the SPOT sensors. The median over the 10 calibration ESUs is represented in solid thick line. The dashed lines represent two contrasted units: U04(■) and U05 (♦). On the top of the figure, the dates of satellite sensors acquisition are given: SPOT (■), ERS (♦) and Radarsat (♦).

**Radiometric calibration.** Particular attention was paid to the radiometric calibration of the SPOT images in order to get accurate and consistent top of atmosphere radiances. In addition, atmospheric correction was applied using the SMAC code (Rahman and Dedieu, 1994) fed with the CIMEL automatic sun-photometer installed in the vicinity of the experimental site. The CIMEL sunphotometer was connected to the AERONET network (Hoblen et al., 1998). The quality of the SPOT time series may be evaluated in more detail. It is possible to show a wide range of sources of variation such as atmosphere and haze residual effects, soil moisture effects due to rainfall events just before the SPOT overpass, view angle variation, as well as possible residual calibration error between HRV instruments. For the SAR sensors, back-scattering coefficients ( $\sigma^{\circ}$ ) were derived using algorithms developed by the European and Canadian Space Agencies (Laur et al., 1992; Shepherd and Srivastava, 1997).

The spatial sampling scheme used will first be presented. Then the ground measurements will be described with illustration by few results.

### 2.4.1. Selection of the elementary sampling units

All the ground measurements were made over elementary sampling units (ESU) that could be easily matched with a small group of  $20 \times 20 \text{ m}^2$  pixels derived from the satellite images. An elementary sampling unit was thus roughly corresponding to  $30 \text{ m}^2$  diameter area. Each ESU was placed at a minimum of 50 m from a border to avoid any problems due to possible mis-registration of the images. The center of each ESU was accurately geo-referenced thanks to a differential GPS device. During the campaign 2000-2001, 42 sampling units were sampled. Their location is presented on figure 1. The selection was achieved by combining several possible factors of variation

Table 2. Distribution of the ESUs as a function of the *a priori* factors of variation.  
The calibration ESUs are indicated in bold face

Cultivars	Precedent crop	Micro-topogr.	Nitrogen	Elementary sampling units (ESU)
Dropia	Favourable	Crov	N+	<b>U08</b> ; U13; U32
			N-	<b>U02</b>
		Flat	N+	<b>U01</b> ; U11; U12; U20; U23; U25; U33; U34; U35
			N-	<b>U09</b>
	Unfavourable	Crov	N+	<b>U04</b> ; U17; U18
			N-	-
		Flat	N+	<b>U05</b> ; U24
			N-	-
Flamura 85	Favourable	Crov	N+	<b>U10</b> ; U16; U19; U21; U29; U30
			N-	U43
		Flat	N+	<b>U03</b> ; <b>U07</b> ; U14; U15; U22; U31; U36
			N-	U42
	Unfavourable	Crov	N+	<b>U06</b> ; U28; U37; U38; U39; U40
			N-	-
		Flat	N+	U26; U27
			N-	-

(Table 2) including: the cultivar, the precedent crop (favourable: pea, chick pea, soybeans, alfalfa; unfavourable: wheat, barley, maize, sunflower), micro-topography (ESU located on „crov” or over a ‘flat’ area) and the nitrogen fertilization (N+: fertilization level satisfactory; N-: limitation in nitrogen fertilization).

Among the 42 ESUs, 10 will be used for the calibration of the process models and tuning of the radiative transfer model inversion techniques. The other 32 ESUs will be dedicated to the validation of these models.

The calibration units were selected to well represent the combination of the factors of variation (Table 2). The difference between the calibration and the validation units consisted mainly in the type and frequency of the measurements. The selection of the sampling units was performed very early in the campaign, just after the localization of the wheat fields, to get the soil initial characteristics. Consequently, the sowing date that was however within a 15 days range was not explicitly used for ESU selection.

#### 2.4.2. Soil measurements

Permanent and dynamic soil variables have been measured over the 42 ESUs. The permanent variable measurements were achieved using classical methods that are described in detail on the web server. Figure 4 shows that the profiles of texture, dry bulk density and moisture at

wilting point are vertically homogeneous. Conversely, the organic matter content shows a decrease with depth. The dispersion observed between ESUs appears to be very small, confirming the low spatial variability associated to this area. The same applies to the chemical characteristics. All these results were very consistent with the findings of Canarache (2002).

In addition to the permanent characteristics, measurements of dynamic variables were also performed. This concerned:

**Surface soil moisture** that was measured using gravimetric techniques. This was achieved mainly during the SAR overpasses to evaluate the accuracy with which soil moisture is estimated from SARs. Some preliminary results will be presented later. Additionally, soil roughness was measured at two periods on few ESUs to sample the possible dynamics due to rainfall. This can be used as input into soil backscattering coefficient model.

**Water moisture and nitrogen profiles** were measured using classical methods at the emergence, anthesis and harvest of the wheat crop. It will allow evaluating the capacity of process models to describe the water and nitrogen balance.

#### 2.4.3. Canopy characterization

Structure measurements used as input into radiative transfer models and biomass measurements were performed on the 42 ESUs.

relatively good temporal consistency for a given unit, indicating the good performances of the methodology used.

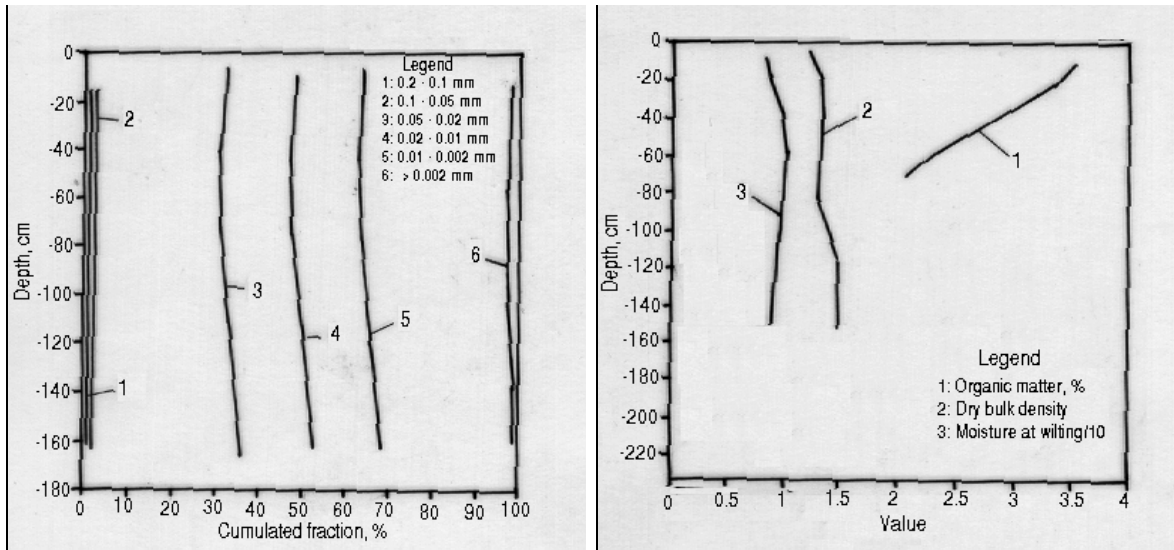


Figure 4. Soil physical properties as observed (on the left) over the 42 sampling units for the texture and (on the right) for organic matter, dry bulk density and moisture at wilting point as observed over the 8 soil profiles sampled

**Structure measurements.** These include dimensions of the stems and leaves, the leaf area index, as well as the number of stems per plants and leaves per stem. The specific leaf weight was measured on this sample by weighing (fresh and dry) the green leaves after measuring the corresponding area. These measurements were achieved on a monthly basis over the 10 calibration units. For each ESU and date of measurement, the sampling used was achieved using three replicates of 2 to 4 plants. Additionally, hemispherical photographs were also taken to be able to describe *in situ* the canopy architecture.

**Biomass.** The biomass measurements were achieved on about 10 day basis for the 10 calibration units, and on a monthly basis for the 32 validation units. The sample used corresponded to 3 to 4 replicates of 0.5 m by two adjacent rows located randomly within the ESU. The fresh biomass was measured extensively on all the replicates. Then a sub-sample of 10 stems was extracted from each replicate to perform detailed biomass distribution and moisture. This includes the green leaf, the senescent leaves, the stems and the ears. Figure 5 shows the variability between the different units as well as the

**Additional measurements.** These include:

- yield and its components (plant density, tillering coefficient, number of grains per ear, and weight of 1000 grains),
- nitrogen content of the leaves, the stems and the plants were measured over fewer ESUs and occasions using the Kjeldhal method. Concurrently, leaf chlorophyll content was measured *in situ* using the Minolta SPAD502 device (Markwell et al., 1995) over at least 30 leaves for each unit and date.

The relationship between the SPAD readings and the chlorophyll content was calibrated using leaf chlorophyll content measured independently using fresh chemistry techniques (Lichtenthaler and Wellburn, 1983).

#### 2.4.4. Yield maps

Yield maps were generated thanks to yield monitor systems connected to GPS devices installed over the combine harvesting machines. They were used over a large fraction of the wheat fields within the area investigated. A dedicated processing was applied to the data to smooth out local problems due to uncertainties in the combine tracks, as well as the delay be-



tween the GPS measurement and the actual location of the grain harvested.

the files except images are „ascii” files that could be easily read by any

Table 3. Organization of the ADAM database

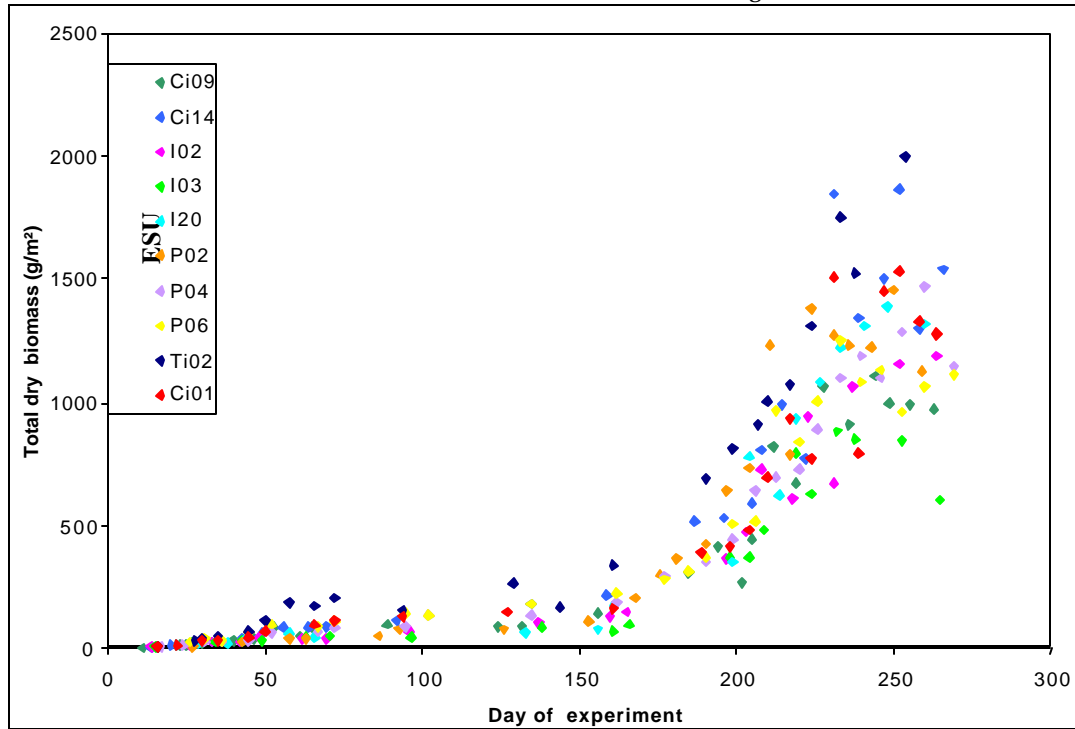


Figure 5. Dynamics of the total dry biomass as observed over the 10 calibration units. Day of experiment is counted since the 23<sup>rd</sup> of September, i.e. day 101 is the first of January 2001

**3. The ADAM data base**

A web-server at [www.medias.mip-obs.fr/adam](http://www.medias.mip-obs.fr/adam) provides an overall description of the ADAM project and the associated measurements available. For this purpose, a database was generated to organize and store the whole set of measurements collected. The main ideas behind the development of this database were directed towards an easy access by any scientist to the data. Apart from the actual accessibility of the data, this forces to provide enough pertinent information on the content of the database, the way it is organized, the format of the data, and the documentation allowing to understand how the measurements have been performed and later processed.

An ftp server hosted at [ftp.medias.mip-obs.fr/adam](ftp://ftp.medias.mip-obs.fr/adam) was set up. It allows freely downloading the data. The database is organized as a hierarchical one according to table 3.

Each directory is documented using a welcome.msg file that pops up when clicking on it, providing the basic information on the content and organization of the data in the directory. All

Satellite	SPOT ERS RadarSat	
	Others	ASTER HYPERION
Meteo-atmosphere	Campbel PAR	
Maps	Control points Sampling units Pedology Geology Yield	
Soil	Permanent characteristics	Physical Chemical
	Profiles	Description Density
	Moisture - nitrogen	Profiles moisture Surface moisture Profiles nitrogen
Vegetation	Roughness Albedo Biomass-LAI Yield Structure Hemispherical photos Chlorophyll Nitrogen Stages-weeds-pests Cultural practices	

Papers-reports	Articles Presentations Reports
----------------	--------------------------------------

work sheet or code. Images have been stored in classical formats that are compatible with most image processing and GIS systems.

#### 4. Sample results

This section will briefly present few results that illustrate the potentials of this database for developing and evaluating methods for crop characterization from high temporal revisit frequency.

##### 4.1. Calibration of the cloud model over ERS and RadarSat data

Surface soil moisture estimation from radar images was investigated in the framework of the semi-empirical „water-cloud” model (Attema and Ulaby, 1978). Previous studies (Prévoit et al., 1993) have shown that in C-band and at low incidence angles, the signal backscattered by the canopy can be neglected, leading to a linear form of the „water-cloud” model when the backscattering coefficient recorded by SAR,  $\sigma^\circ$ , is expressed in dB:

$$\sigma^\circ = C + D m_s - B m_v / \cos \theta$$

where:  $m_s$  is the volumetric surface soil moisture,  $m_v$  is the water content of the vegetation ( $\text{kg H}_2\text{O} / \text{m}^2$ ) and  $\theta$  is the incidence angle. Parameter  $B$  represents the radar signal attenuation by the vegetation layer, whereas the soil parameters  $C$  and  $D$  respectively represent the intercept and the slope (sensitivity) of the linear

relationship between the signal backscattered by a bare soil and its volumetric surface soil moisture.

The model parameters were firstly calibrated using the data acquired over the 10 calibration units, using the following assumptions: (1) the sensitivity to soil moisture  $D$  was assumed to be constant (same for ERS and RadarSat); (2) the attenuation parameter  $B$  was assumed to depend only on the polarization ( $B_{\text{HH}} < B_{\text{VV}}$ ); (3) the intercept  $C$ , which accounts for the effect of the soil roughness, was assumed to depend on the unit considered, on the polarization and implicitly on the incidence angle. Because of the relatively homogeneous character of the soil, the within field variability was small: the within-field variability of the backscattering coefficients was around 1.5 dB. This allowed to average the backscattering coefficients,  $\sigma^\circ$ , over the field level to reduce the effect of the speckle.

Results (Figure 6) show good performances of the cloud model both for ERS (rms = 1.3 dB) and slightly lower performances for RadarSat (rms = 3.8 dB). This might be related to the development of the wheat canopy, since ERS images were mainly acquired at the beginning of the crop cycle, whereas RadarSat images were acquired on fully developed canopies.

The calibrated water-cloud model was then applied to the data acquired over the 32 validation units, the parameter  $C$ , which represents the effect of the soil roughness, being calculated for each unit and each polarization. The accu-

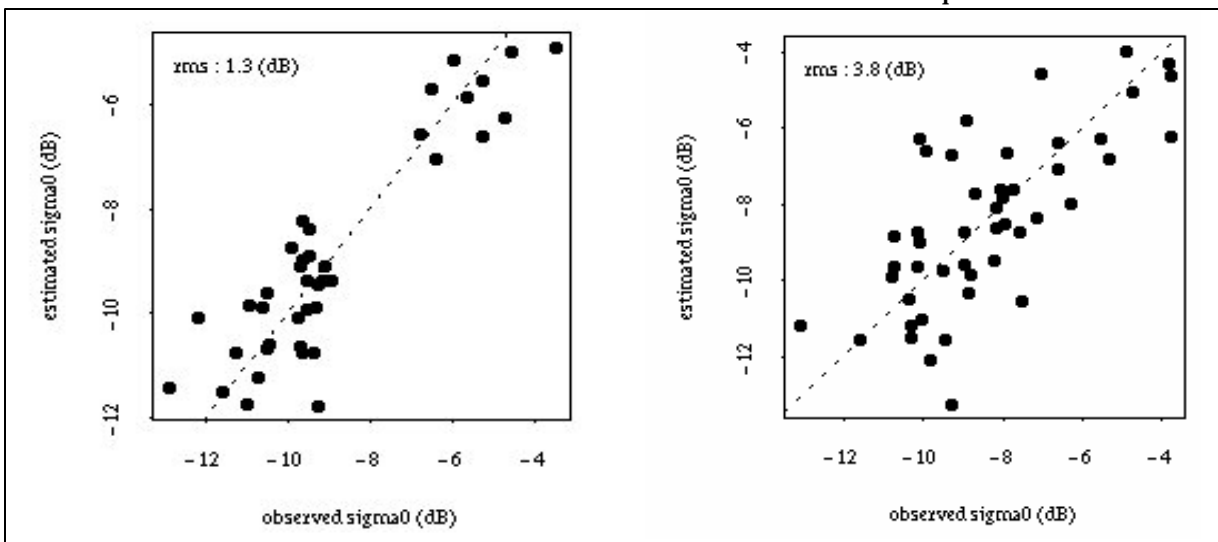


Figure 6. Comparison between the  $\sigma^\circ$  simulated thanks to the cloud model and the measured soil moisture and plant water content and that measured from ERS (left) or RadarSat (right). Results observed over the 10 calibration units

racy obtained during this calibration phase is 0.2 dB for the ERS data and 0.5 dB for the RadarSat data.

Further work will be carried out for producing surface soil moisture maps through application of the water-cloud model, the water content of the canopy being estimated at each SAR acquisition date from SPOT images.

#### 4.2. LAI dynamics

The leaf area index, LAI, is the main biophysical canopy variable that can be extracted from remotely sensed data. LAI is involved in several canopy functioning processes, such as photosynthesis and evapotranspiration. To get continuous estimates of LAI for forcing crop functioning models, an evaluation of the use of a semi-empirical dynamic model was performed. Note that this dynamic model of LAI (called MODLAI) could be also used to smooth out estimates of LAI from remote sensing reflectance measurements. In a first step, the MODLAI model was fitted over the 10 calibration units to derive estimates of LAI at the time of SPOT data acquisition.

Then, empirical transfer functions were developed for each individual SPOT date, based on multiple regression between LAI (dependant variable) and the top of canopy

reflectance ( $r_b$ ) as observed in the three first SPOT bands (XS1: green, XS2: red, and XS3: near infrared):

$$LAI = a_0 + \sum_{b=1}^3 a_b r_b + e$$

where:  $\alpha_0$  and  $\rho_b$  are coefficients and  $\varepsilon$  the residual error.

Figure 7 shows the relatively good performances of the empirical transfer functions, particularly for the early stages where the sensitivity of reflectance to LAI is maximal. Then the performances decrease, presumably because of the saturation effects observed for the larger LAI values.

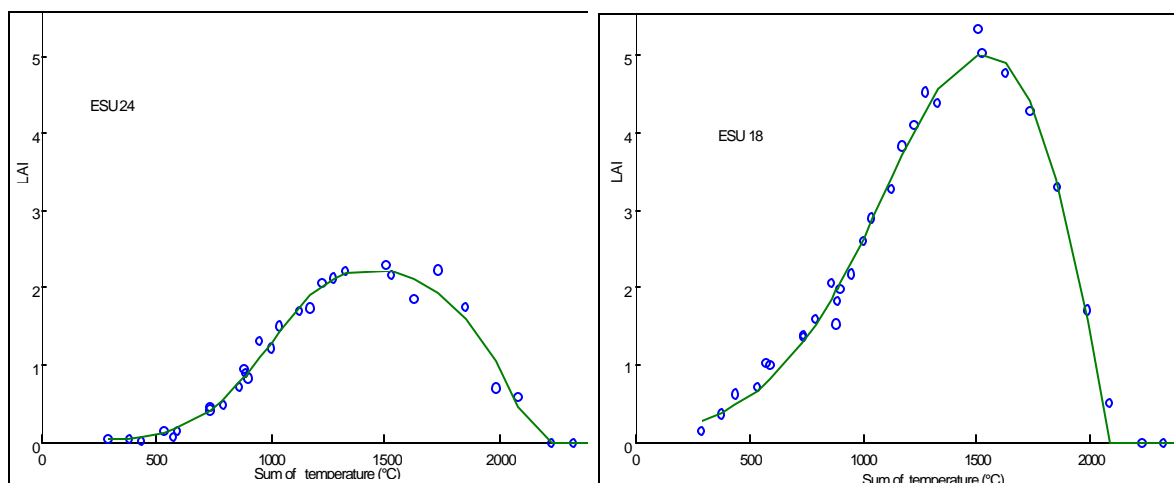


Figure 8. Two examples of contrasted validation units dynamics. The circles correspond to the LAI estimated from SPOT data thanks to the empirical transfer function. The solid line corresponds to the MODLAI model fitted over the SPOT LAI estimates

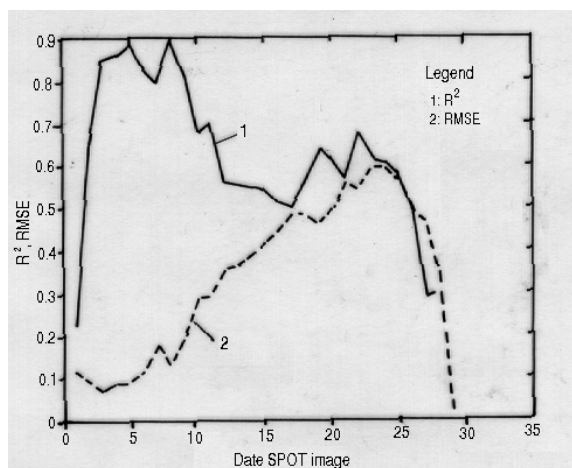


Figure 7. Performances of the empirical transfer function over the 10 calibration units

Subsequently, the transfer functions were used to extend the local measurements made over the calibration units to the ensemble of pixels corresponding to wheat crops.

Results (Figure 8) show the good performances of the approach. This will be further investigated, with application to the forcing of canopy functioning models for yield, carbon, water and nitrogen fluxes and storage estimation. It will be also used to better define the optimal temporal sampling strategy for remote sensing observations.

## CONCLUSION AND PERSPECTIVES

The ADAM project is aiming at the development and evaluation of methods capable of exploiting high revisit frequency and high spatial satellite observations. The intensive experimental campaign conducted in 2000-2001 over wheat crops yielded a unique database, where frequent satellite observations at high spatial resolution in the solar and microwave domains were made concurrently to ground characterization of the soil, the canopy and their functioning. This intensive campaign described in this paper will be followed in 2002 and 2003 by lighter campaigns where a reduced number of ESUs will be sampled and a reduced number of SPOT scenes will be acquired.

This unique database and experiment offered already the opportunity to investigate the quality of the SPOT sensors as instruments for the quantitative monitoring of canopies. They

show good performances in terms of programming and accessibility thanks to the use of three satellites, the de-pointing capacity and swath. However, this experiment highlighted the great attention to pay to the pre-processing of the radiometric data to get a consistent time series. More emphasis should be put on the development of automatic co-registration systems, automatic atmospheric correction schemes, either based on autonomous correction or using ancillary information possibly provided by medium resolution sensors. Finally, inter-calibration between sensors appears also a critical issue that should not be neglected.

The ADAM database has been already been partly exploited. The preliminary results obtained showed good prospects, indicating that the measurements were accurate and consistent enough. However, the potentials of exploitation of this database are very high. Ongoing studies on the assimilation of remote sensing data into canopy functioning models (Lauvernet et al., 2003) will provide information on the use of high revisit frequency observations. It will also provide some results on the optimal temporal sampling. The intensive ground measurements have already yielded some interesting results on the crop growth modeling, and investigations are still on going to better describe the interaction between the soil, the plant, and the climate, without forgetting the human action through cultural practices. Apart from the applications and associated questions posed at the high spatial resolution, this database offers also good potentials for investigating scaling problems with possible use for the regional scale and exploitation of medium resolution sensors. We hope that the accessibility of the ADAM database permit its intensive exploitation which should ultimately foster the advancement of the use of remote sensing data for crop monitoring, and promote synergistic cooperation between scientists.

## Acknowledgements

*The ADAM Project is supported by the French Space Agency (CNES) as well as INRA and ESAP in France, and by the Romanian Space Agency, RISSA*

**and RICIC in Romania. It was made possible thanks to the participation of many people both from Romania and France, and very warm thanks have to be directed towards them. They were: I. Piciu, E. Gamenz (RISSA Bucharest), A. Arsintescu, G. Gărgăriță (RICIC Fundulea), F. <sup>a</sup>erban, A. Badea (ASR Bucharest), R. Mudura (Cruta) and O. Balota (Intergis srl).**

## REFERENCES

- Attema, E.P.W. and Ulaby, F.T., 1978. Vegetation modeled as a water cloud. *Radio Science*, 13(2): 357-364.
- Canarache, A., 2002. A Soil-Management-Yield System: Case Study in Fundulea-Ileana area. *Romanian Soil Science Journal*, XXXVI(1): 20-32.
- Dedieu, G., Cabot, F. and Leroy, M., 1999. Proposition de mission actualisée. RHEA, CESBIO/CNES, Toulouse (France).
- Holben, B.N., Eck, T.F., Slutsker, I., Tanré, D., Buis, J.P., Setzer, A., Vermote, E., Reagan, J.A., Kaufman, Y.F., Nakajima, T., Lavenue, F., Jankowiak, I. and Smirnov, A., 1998. AERONET -A federal instrument network and data archive for aerosol characterization. *Remote Sensing of Environment*, 66: 1-16.
- Laur, H., Bally, P., Meadows, P., Sanchez, J., Schaettler, B. and Lopinto, E., 1992. Derivation of the backscattering coefficient in ESA ERS SAR PRI Products. ES-TN-RS-PM-HL09, Issue 2, Rev. 4, European Space Agency.
- Lichtenthaler, H.K. and Wellburn, A.R., 1983. Determination of total carotenoids and chlorophylls a and b of leaf extracts in different solvents. *Biochemical Society Transactions*, 603: 591-592.
- Markwell, J., Osterman, J.C. and Mitchell, J.C., 1995. Calibration of the Minolta SPAD-502 leaf chlorophyll meter. *Photosynthesis Research*, 46: 467-472.
- Prévo, L., Champion, I. and Guyot, G., 1993. Estimating surface soil moisture and leaf area index of a wheat canopy using a dual frequency (C and X band) scatterometer. *Remote Sensing of Environment*, 46: 331-339.
- Rahman, H. and Dedieu, G., 1994. SMAC: a simplified method for the atmospheric correction of satellite measurements in the solar spectrum. *International Journal of Remote Sensing*, 15(1): 123-143.
- Rast, M., Del Bello, U., Baret, F., Menenti, M., Schimel, D.S. and Verstraete, M., 2001. SPECTRA: Surface Processes and Ecosystem Changes Through Response Analysis. SP-1257 (5), ESA/ESTEC, Noordwijk (The Netherlands).
- Shepherd, N. and Srivastava, S., 1997. Extraction of beta nought and sigma nought from RadarSat CDPF Products. 9F005-6-0025/001/SN, CSA Document.

**Table 1. Influence of aluminum ions, in reaction mixture, on the level of saccharasic activity in a reddish-brown soil fertilized with compost with different quantities (glucose+fructose-mg/100 g soil dw/24 hours)**

A- Factor	B – Factor – COMPOST (t/ha)								Average (A)	
	b1-0	%	b2-0	%	b3-0	%	b4-0	%		%
a1–without Al <sup>3+</sup>	b 3287	100	b 4028	100	b 2579	100	b 3472	100	b 3341	100
a2- with Al <sup>3+</sup>	a 4228	129	a 5019	125	a 3472	135	a 4528	130	a 4312	129
Average (B)	3757 c		4523 a		3025 d		4000 b			
LD P	5%	1%	0,1%							
A	291	673*	2143							
B	101	142	201*							
AB	302	628*	1799							
BA	144*	201	284							

**Table 2. Influence of aluminum ions, in reaction mixture, on the level of saccharasic activity in a chernozem mineral fertilized or manured with farmyard compost (glucose+fructose-mg/100 g soil dw/24 hours)**

A- Factor	B – Factor – COMPOST (t/ha)										Average (A)	
	b1-0	%	b2-N <sub>32</sub> P <sub>32</sub>	%	b3-N <sub>94</sub> P <sub>96</sub>	%	b4-N <sub>128</sub> P <sub>128</sub>	%	b5 com-post	%		%
a1–without Al <sup>3+</sup>	b 1564	100	b 1496	100	b 1459	100	b 1401	100	b 1732	100	b 1530	100
a2- with Al <sup>3+</sup>	a 1686	108	a 1581	106	a 1684	115	a 1589	113	a 1864	108	a 1681	110
Average (B)	1625 b		1538 d		1571 c		1495 e		1798 a			
LD P	5%	1%	0,1%									
A	7	17	54*									
B	14	20	27*									
AB	19	28	45*									
BA	20*	28	39									

## ROMANIAN AGRICULTURAL RESEARCH

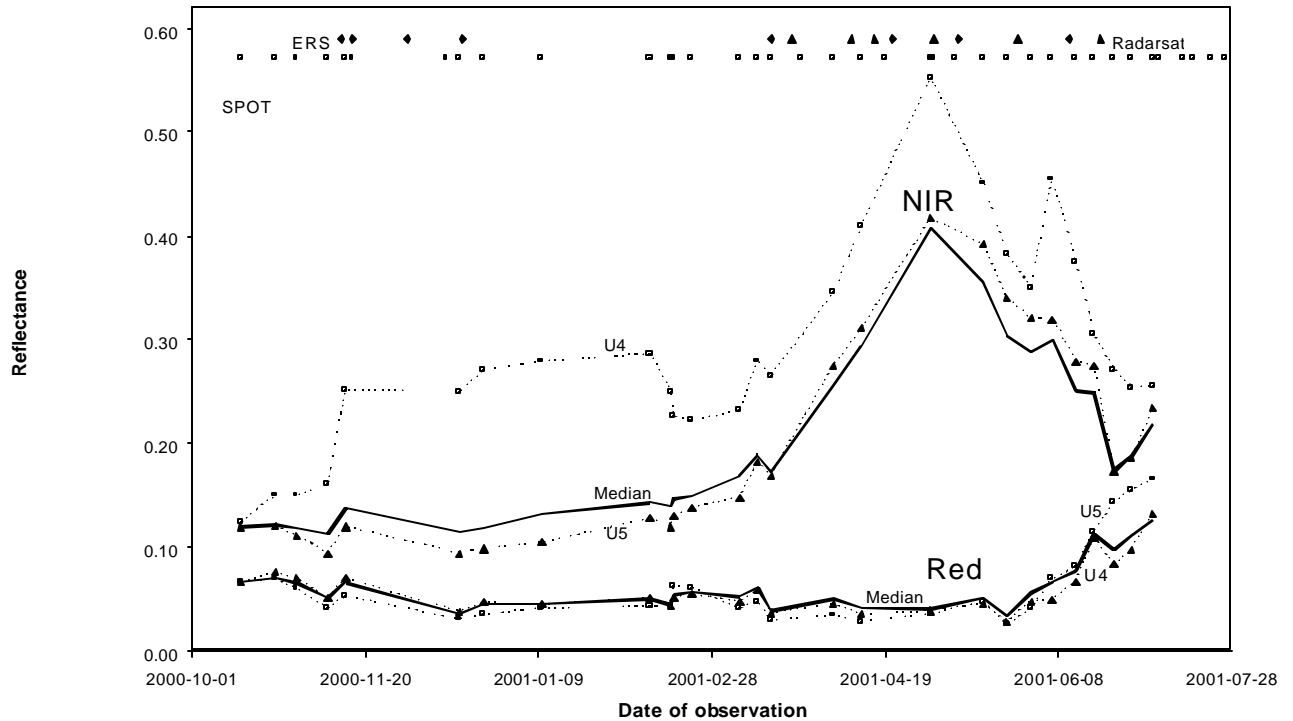


Figure 3. Temporal sampling of satellite observations over the ADAM site. The bottom graphs correspond to the red (Red) and near infrared (NIR) top of canopy reflectance as derived from the SPOT sensors. The median over the 10 calibration ESUs is represented in solid thick line. The dashed lines represent two contrasted units: U04(■) and U05 (♦). On the top of the figure, the dates of satellite sensors acquisition are given: SPOT (■), ERS (♦) and RadarSat (♦).

Table 1. Main characteristics of the satellite instruments used during the ADAM experiment

Sensor	Satellite	Number of bands & spectral domain	Spatial sampling	Revisit frequency	Swath width	View zenith angle	Polarization
HRV-XS	SPOT 1 SPOT 2	VNIR (3)	20 m	3 days	60 km	$\pm 27^\circ$ across-track	no
HRVIR	SPOT 4 SPOT 5	VNIR (3) SWIR (1)					
ERS 2		C-band	20 m	16 days	100 km	$23^\circ$	VV
RADARSAT		C-band	20 m	24 days	170 km	$16^\circ$	HH

Table 2. Distribution of the ESUs as a function of the "a priori" factors of variation.

The calibration ESUs are indicated in bold face.

Cultivar	Precedent	Micro-topogr.	Nitrogen	Elementary sampling units (ESU)
'Dropia'	Favorable	'Crov'	N+	<b>U08</b> ;U13;U32
			N-	<b>U02</b>
	Flat		N+	<b>U01</b> ;U11;U12;U20;U23;U25;U33;U34;U35
			N-	<b>U09</b>

	Unfavorable	'Crov'	N+	<b>U04;U17;U18</b>
			N-	-
	Flat	N+	<b>U05;U24</b>	
		N-	-	
'Flamura 85'	Favorable	'Crov'	N+	<b>U10;U16;U19;U21;U29;U30</b>
			N-	U43
	Flat	N+	<b>U03;U07;U14;U15;U22;U31;U36</b>	
		N-	U42	
	Unfavorable	'Crov'	N+	<b>U06;U28;U37;U38;U39;U40</b>
			N-	-
	Flat	N+	U26;U27	
		N-	-	

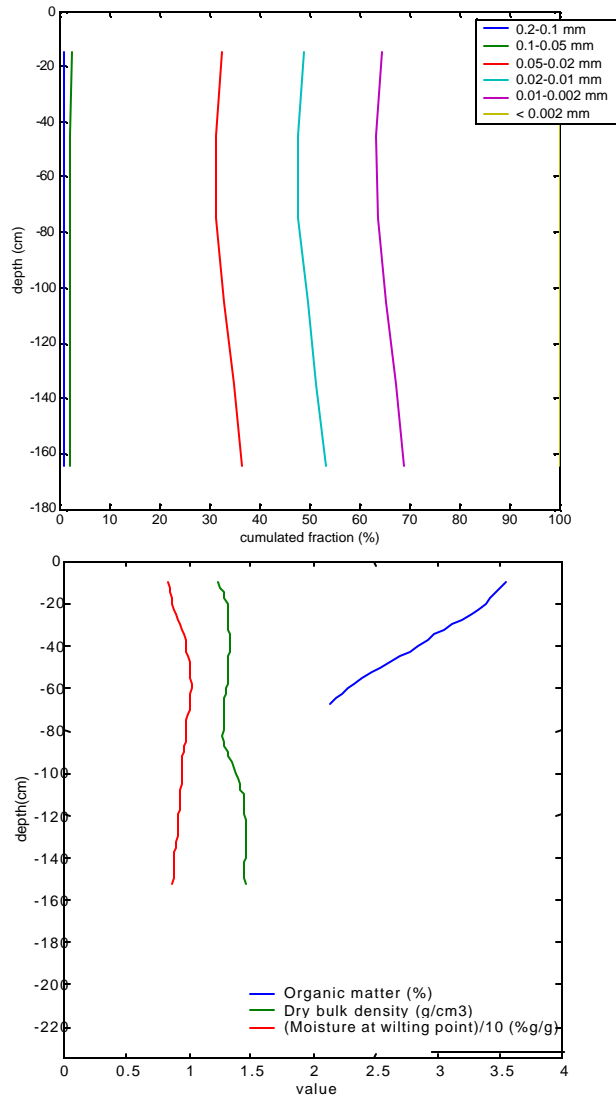


Figure 4. Soil physical properties as observed (on the left) over the 42 sampling units for the texture and (on the right) for organic matter, dry bulk density and moisture at wilting point as observed over the 8 soil profiles sampled



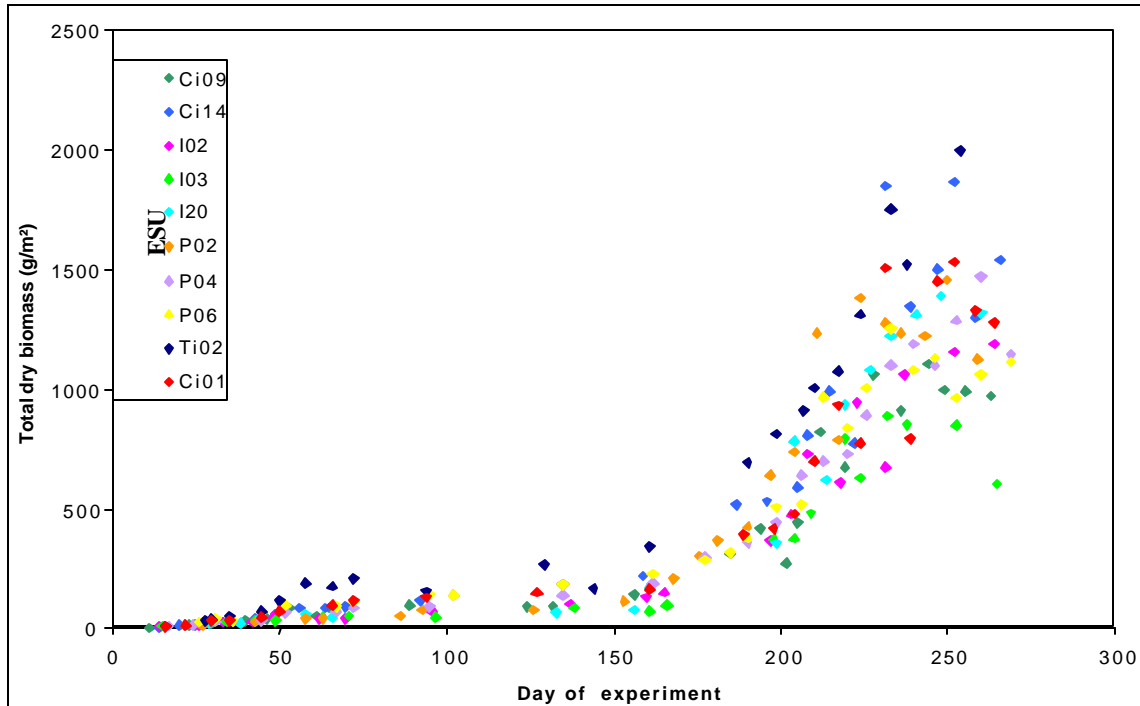


Figure 5. Dynamics of the total dry biomass as observed over the 10 calibration units. Day of experiment is counted since the 23rd of September, i.e. day 101 is the 1st of January 2001.

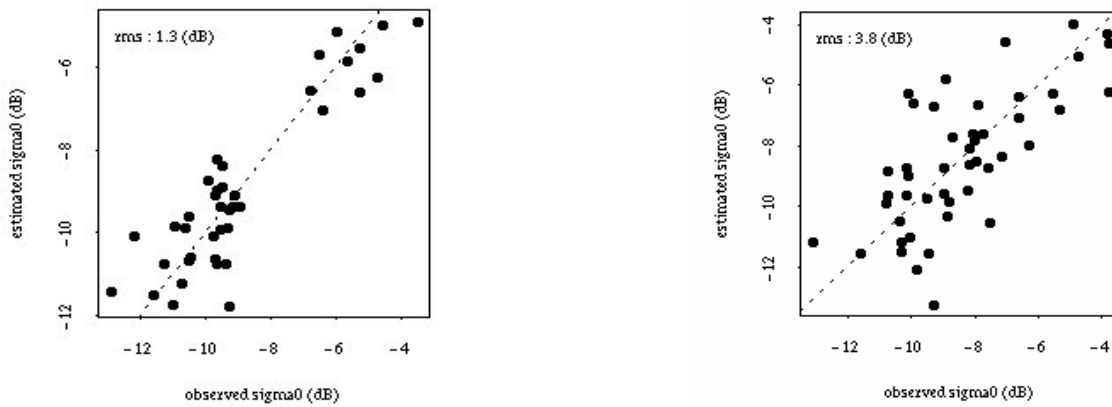
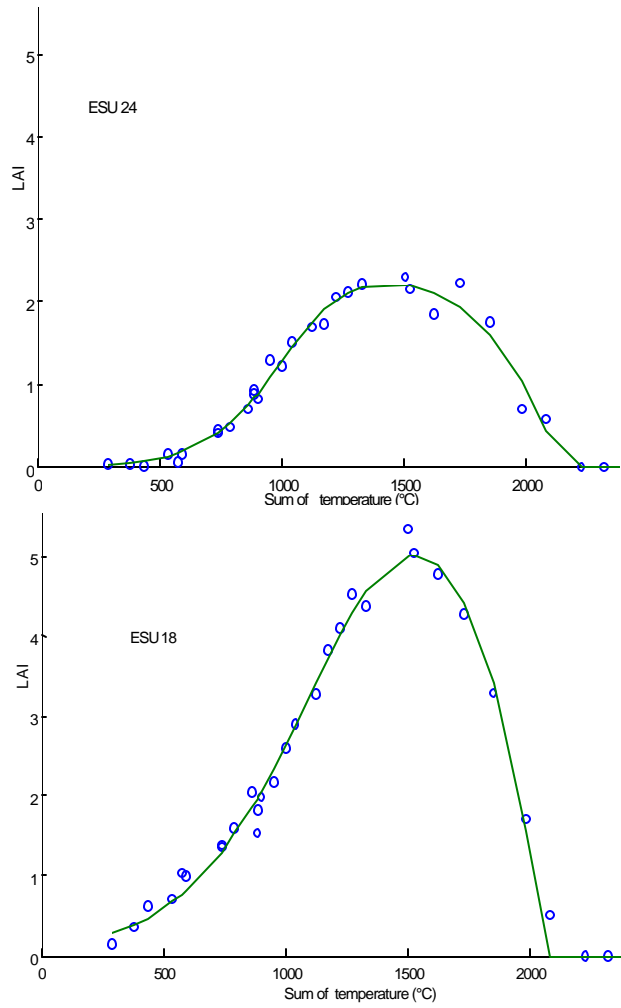


Figure 6. Comparison between the  $\sigma^0$  simulated thanks to the cloud model and the measured soil moisture and plant water content and that measured from ERS (left) or RadarSat (right). Results observed over the 10 calibration units.



**Figure 8.** Two examples of contrasted LAI dynamics over validation units. The circles correspond to the LAI estimated from SPOT data thanks to the empirical transfer function. The solid line corresponds to the MODLAI model fitted over the SPOT LAI estimates